

# Dynamical constraints on the neutron star mass in EXO 0748-676

T. Muñoz-Darias<sup>1</sup>\*, J. Casares<sup>1</sup>, K. O’Brien<sup>2</sup>, D. Steeghs<sup>3,4</sup>, I. G. Martínez-Pais<sup>1,5</sup>,  
R. Cornelisse<sup>1</sup>, and P. A. Charles<sup>6</sup>

<sup>1</sup> *Instituto de Astrofísica de Canarias, 38200 La Laguna, Tenerife, Spain*

<sup>2</sup> *European Southern Observatory, Casilla 19001, Santiago 19, Chile*

<sup>3</sup> *Dept. of Physics, Univ. of Warwick, Coventry CV4 7AL, UK*

<sup>4</sup> *Harvard-Smithsonian Center for Astrophysics, Cambridge, MA 02138, USA*

<sup>5</sup> *Departamento de Astrofísica, Universidad de La Laguna, E-38206 La Laguna, Tenerife, Spain*

<sup>6</sup> *South Africa Astronomical Observatory, P.O. Box 9. Observatory 7935, South Africa*

10 September 2021

## ABSTRACT

We present VLT intermediate resolution spectroscopy of UY Vol, the optical counterpart of the LMXB X-ray burster EXO 0748-676. By using Doppler tomography we detect narrow components within the broad He II  $\lambda 4542$ ,  $\lambda 4686$  and  $\lambda 5412$  emission lines. The phase, velocity and narrowness of these lines are consistent with their arising from the irradiated hemisphere of the donor star, as has been observed in a number of LMXBs. Under this assumption we provide the first dynamical constraints on the stellar masses in this system. In particular, we measure  $K_2 > K_{\text{em}} = 300 \pm 10 \text{ km s}^{-1}$ . Using this value we derive  $1 M_{\odot} \leq M_1 \leq 2.4 M_{\odot}$  and  $0.11 \leq q \leq 0.28$ . We find  $M_1 \geq 1.5 M_{\odot}$  for the case of a main sequence companion star. Our results are consistent with the presence of a massive neutron star as has been suggested by Özel (2006), although we cannot discard the canonical value of  $\sim 1.4 M_{\odot}$ .

**Key words:** accretion disks - binaries: close - stars: individual: EXO 0748-676 - X-rays:stars

## 1 INTRODUCTION

EXO 0748-676 (=UY Vol) is a Low Mass X-ray Binary (LMXB) discovered as a transient source by EXOSAT in 1985 (Parmar et al. 1985). Instead of returning to the quiescent state the system had remained in an active state ever since, showing typical properties of persistent LMXBs. However, it has returned to the off-state very recently (Hynes & Jones 2008).

EXO 0748-676 also exhibits irregular X-ray dips and periodic eclipses which have provided an excellent determination of the orbital period ( $P=3.82$  h) and the orbital inclination ( $i = 75^\circ - 82^\circ$ ; Parmar et al. 1986). On the other hand, Villarreal & Strohmayer (2004) have detected a burst oscillation at 45 Hz during type I X-ray burst events which is associated with the neutron star (NS) spin frequency. Recently, Özel (2006) have suggested the presence of a massive NS with  $M_1 = 2.10 \pm 0.28 M_{\odot}$  and  $R_1 = 13.8 \pm 1.8$  km in EXO 0748-676. This result is based on the gravitational redshift measured in O and Fe absorption lines arising from the surface of the NS (Cottam et al. 2002) and the assumption that the strong thermonuclear X-ray bursts displayed by the system (Gottwald et al. 1986) can be modelled by a phase of symmetric expansion of the NS radius and a cooling phase where the X-ray emission is Eddington-limited. In contrast, Pearson et al. (2006) have reported

He II  $\lambda 4686$  Doppler tomograms which show a spot consistent with the expected gas stream position. These authors favor a NS of  $1.35 M_{\odot}$  by fitting different gas stream trajectories to the position of the spot.

In this paper we present VLT-FORS1 spectroscopy of the  $V \sim 17$  optical counterpart (UY Vol) of EXO 0748-676 which reveals the presence of narrow emission components within the He II emission lines. In recent years, narrow emission lines from the donor have been detected in several LMXBs (see Cornelisse et al. 2008 for details, also Casares 2009) since they were first discovered by Steeghs & Casares (2002) in Sco X-1. The Roche lobe filling donor star intercepts the energetic photons from the inner accretion disc resulting in the observed optical emission lines from its surface. The Doppler motion of these lines traces the orbit of the companion star, thereby providing the first constraints on the binary parameters for persistent systems where the photospheric light from the companion is otherwise swamped by the bright accretion disc. It is remarkable that this technique has proved the presence of a black hole with a mass  $> 6 M_{\odot}$  in GX339-4 (Hynes et al. 2003; Muñoz-Darias et al. 2008), presented evidence for a massive NS in Aql X-1 (Cornelisse et al. 2007) and X1822-371 (Casares et al. 2003; Muñoz-Darias et al. 2005), and provided the first constraints on the binary parameters in six other LMXBs, including the prototypical system Sco X-1 (Steeeghs & Casares 2002). In this letter we present the first dynamical constraints on the stellar masses in EXO

\* E-mail: tmd@iac.es

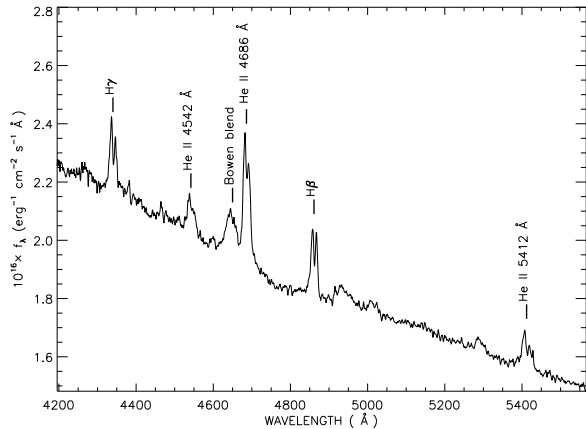


**Figure 1.** Average spectrum of EXO 0748-676 after combining 21 exposures obtained with good seeing conditions ( $\lesssim 0.6$  arc-sec) and out of eclipse. The most prominent lines are indicated for clarity.

0748-676 based on the study of the narrow components present within the He II  $\lambda 4541$ ,  $\lambda 4686$  and  $\lambda 5412$  emission profiles. In section 2 we describe the observations and data reduction process, whereas the data analysis is presented in section 3. Results are discussed in sections 4 and 5.

## 2 OBSERVATIONS AND DATA REDUCTION

We observed EXO 0748-676 on 22 Jan 2008 using the *Focal Reducer and low dispersion Spectrograph-1* (FORs1) attached to the VLT-UT2 (Kueyen) telescope at the Observatorio Astronómico Cerro Paranal (Chile). We used the GRIS\_1200g holographic grating obtaining a total of 28 spectra of 600s each. The slit width was fixed at 0.51-arcsec resulting in a spectral resolution of  $\sim 90$  km s $^{-1}$  and a wavelength coverage of  $\lambda\lambda 4185 - 5600$  Å. The seeing stayed between 0.4-0.6-arcsec during the first 4 hours but it increased up to 1-arcsec during the last hour of the run, making slit losses significant and absolute flux calibration unreliable for this part of the night. In total we covered  $\sim 1.3$  binary orbits (i. e.  $\sim 5$  h of data). The images were de-biased and flat-fielded and the spectra extracted using conventional IRAF routines. The wavelength calibration was performed by fitting a fourth-order polynomial to an arc image taken during daytime. This resulted in a dispersion of  $0.73$  Å pix $^{-1}$  and rms scatter  $\leq 0.04$  Å. We used the sky spectra to correct for velocity drifts due to instrumental flexure which were found to be  $\leq 10$  km s $^{-1}$  (i. e.  $\leq 0.25$  pix). The zero point of the wavelength scale was established from the position of the strong OI  $\lambda 5577.338$  sky-line. The spectra were finally flux calibrated using observations of the flux standard LTT 1788 and exported into our analysis software (MOLLY).

## 3 DATA ANALYSIS

Fig. 1 shows the average spectrum of EXO 0748-676. In order to produce this figure we used the 21 out-of-eclipse spectra taken with good seeing conditions, comparable to the slit-width. The H $\gamma$  and H $\beta$  double peak emission lines together with the strong He II  $\lambda 4542$ ,  $\lambda 4686$ ,  $\lambda 5412$  features and the Bowen blend at  $\lambda\lambda 4630 - 50$  are clearly seen in the spectrum. He I  $\lambda 4922$ ,  $\lambda 5016$ , and Fe II  $\lambda 5284$  are also detected, although they are less prominent.

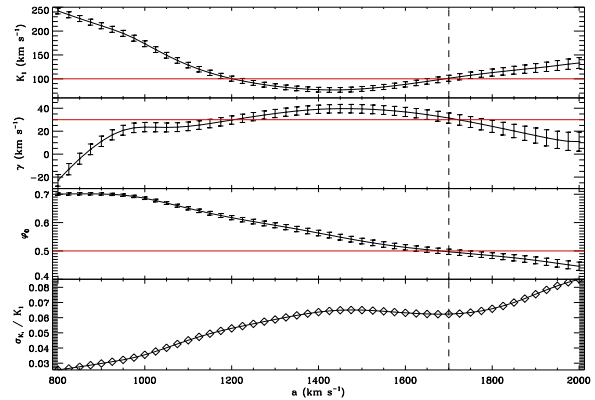


**Figure 2.** Diagnostic diagram of He II  $\lambda 4686$  obtained by fitting eq. 1 to the radial velocity curves extracted for each value of the Gaussian separation  $a$ . The vertical dashed line shows the selected value for  $a$  and the horizontal lines the values adopted for each parameter.

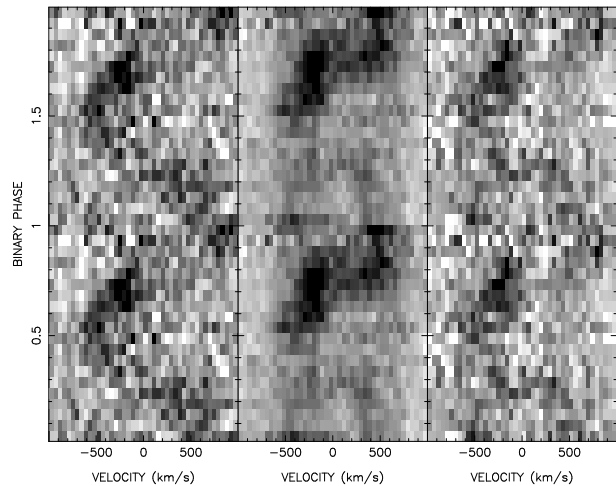


**Figure 3.** Triled spectra showing the orbital evolution of the emission lines He II  $\lambda 4542$ ,  $\lambda 4686$  and  $\lambda 5412$  (from left to right) in 20 phase bins. Two orbital periods have been plotted for clarity.

In this paper we will focus on the analysis of the He II emission lines where narrow components are found. In order to compute the orbital phase of each spectrum we used the constant-period ephemeris given by Wolff et al. (2002). The zero-phase has been refined by fitting the mid-eclipse time of an eclipse observed by RXTE on 30 Jan 2008 (i.e. only 8 days after our observations). We find an error of  $\sim 0.012$  in orbital phase which has been corrected in the ephemeris. We finally adopted:

$$T_0(HJD) = 2446111.57285(3) + 0.1593378191(1) \times N$$

### 3.1 Systemic velocity

As in our previous work, we decided to apply the double gaussian technique (Schneider & Young 1980) to the wings of the He II  $\lambda 4686$  emission line in order to obtain a first estimate of the orbital parameters of the NS. We have used relative Gaussian separations between  $a = 800 - 2000$  km s $^{-1}$  in steps of 25 km s $^{-1}$ .

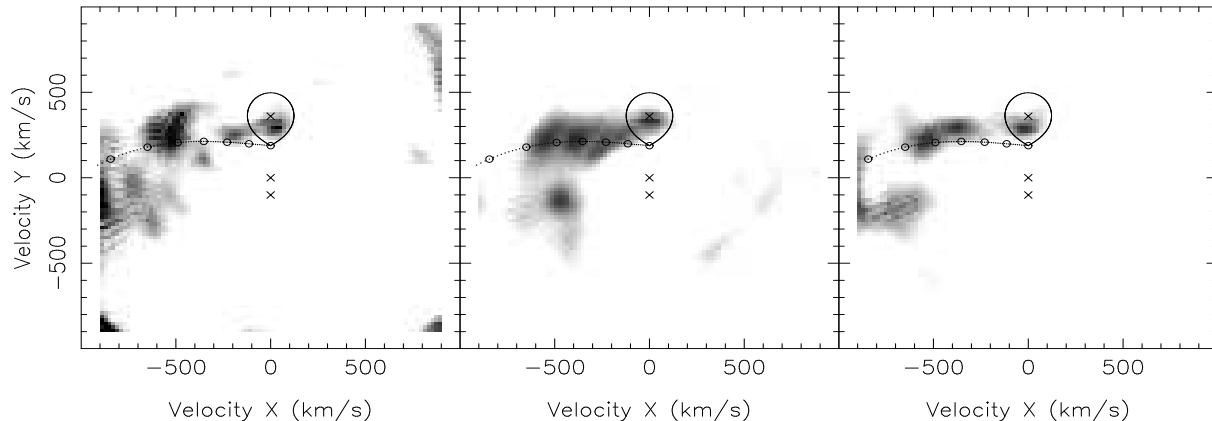


**Figure 4.** Doppler maps corresponding to He II  $\lambda 4542$ ,  $\lambda 4686$ ,  $\lambda 5412$  (from left to right) computed using our refined ephemeris. A systemic velocity of  $\gamma = 70 \text{ km s}^{-1}$  was used for the three cases. We have over-plotted the position of the compact object, the gas stream trajectory and the Roche lobe of the companion star assuming  $K_1 = 100 \text{ km s}^{-1}$  and  $K_2 = 360 \text{ km s}^{-1}$ .

This range has been chosen to avoid low velocity components associated with the companion star and the outer disc. After fitting the expression

$$V(\phi) = \gamma + K_1 \sin 2\pi(\phi - \phi_0) \quad (1)$$

to the radial velocity curves extracted for each value of  $a$ , we obtain the diagnostic diagram presented in Fig. 2. We adopt the value of  $a \sim 1700 \text{ km s}^{-1}$  where the phase is correct and also happens to occur near the plateau in the diagnostic parameter  $\sigma(K_1)/K_1$  (Shafter et al. 1986). This results in  $\gamma = 30 \pm 10 \text{ km s}^{-1}$  and  $K_1 = 100 \pm 20 \text{ km s}^{-1}$ .

This method assumes that the emission line gas orbits the compact object and correctly traces its orbital dynamics. Non-isotropic emission and/or significant disk asymmetries are known to lead to significant distortions in the radial velocity curves and thus the inferred  $K_1$ . For this reason the values provided by the diagnostic-diagram should be taken as a rough approximation to the real ones, as will be discussed in the next section.

### 3.2 Doppler mapping

Extracting radial velocities of faint short-period systems is not straightforward. The situation is even more difficult when dealing with narrow spectral lines which require high spectral resolution. The spectral resolution also degrades with exposure time due to orbital smearing, whereas the signal-to-noise ratio (S/N) obviously increases for longer integrations. Therefore, in order to avoid significant orbital smearing one has to use short exposures (600 s in our case) which results in data sets with good orbital sampling but poor S/N.

Using Doppler tomography (Marsh & Horne 1988) instead of standard radial velocity curves has the benefit of using all the spectra at the same time, allowing one to map the brightness distribution of a weak emission line in velocity space. This method has been used in almost all previous studies of narrow emission lines (see e.g. Casares et al. 2006), and only for Sco X-1 (with  $V \sim 12$  and  $P=18.9$  h) has the application of both techniques separately (i.e. radial velocity curves and Doppler mapping) been possible. In that case a good agreement between the two methods was found (Steehgs & Casares 2002).

Fig. 3 shows the evolution of the He II  $\lambda 4542$ ,  $\lambda 4686$  and  $\lambda 5412$  spectral lines along the orbit. An S-wave with a maximum

radial velocity of  $\sim 500 \text{ km s}^{-1}$  at orbital phase  $\sim 0.5$  appears in the 3 maps. This translates into bright spots at  $V(V_X, V_Y) = (-500, 200) \text{ km s}^{-1}$  in the Doppler maps of the three He II lines (Fig. 4). Similar spots were also found by Pearson et al. (2006) in several emission lines (e.g He II  $\lambda 4686$ ). However, in this study we also detect in the three maps compact spots at the position of the donor (i.e.  $V_X = 0 \text{ km s}^{-1}$ ). The velocities associated with these spots are in the range  $V_Y = 270 - 339 \text{ km s}^{-1}$  and are shown in table 1.

We have computed Doppler maps for a wide range of  $\gamma$  values bracketing  $\gamma = 30 \text{ km s}^{-1}$ , the value favored by the diagnostic diagram. We swept between  $\gamma = -50$  and  $100 \text{ km s}^{-1}$  in steps of  $10 \text{ km s}^{-1}$ . The effect of using a wrong value of  $\gamma$  when computing the maps is to obtain out-of-focus spots, which become compact when approaching the correct value. By fitting 2D Gaussians to the spots as a function of  $\gamma$ , we favor systemic velocities in the range  $20 \leq \gamma \leq 80 \text{ km s}^{-1}$ . We finally selected  $\gamma = 70 \text{ km s}^{-1}$  because it produces significantly more compact spots in the three maps. In any case, the velocity measurements (table 1) derived with  $\gamma = 70 \text{ km s}^{-1}$  are consistent within the errors with those obtained with  $\gamma = 30 \text{ km s}^{-1}$ .

The  $K_{\text{em}}$  velocity of a given irradiation line depends on the disc thickness and how transparent it is for the irradiating photons. The three He II lines that we study here have similar ionization potentials and, hence, one should expect them to show the same  $K_{\text{em}}$  value. This is consistent within the error bars with the results that we have obtained. Therefore, we decided to take the weighted mean value of the three lines as our best estimate of  $K_{\text{em}}$ , which results in  $K_{\text{em}} = 310 \pm 10 \text{ km s}^{-1}$ . Hence, we will use  $K_{\text{em}} = 300 \text{ km s}^{-1}$  as 1-sigma lower limit to  $K_2$ .

## 4 REPROCESSED EMISSION FROM THE COMPANION

Using our  $K_{\text{em}}$  value derived from the He II lines and the refined orbital ephemeris it is possible to remove the orbital velocity from each spectrum and compute the average spectrum in the rest frame of the companion. Fig 5 shows this spectrum, where narrow components standing out in the broad He II  $\lambda 4542$ ,  $\lambda 4686$  and  $\lambda 5412$  emission lines are clearly seen. As an independent test to the Doppler analysis, we have computed the spectrum in the rest frame of the donor sweeping a wide range of  $K_{\text{em}}$  values. We find

**Table 1.**  $K_{em}$  ( $V_X$ ,  $V_Y$ ) measurements ( $\text{km s}^{-1}$ ) in EXO 0748-676.

$\lambda 4542$	He II $\lambda 4686$	He II $\lambda 5412$
$(28, 300) \pm 18$	$(7, 325) \pm 14$	$(-14, 290) \pm 20$

that, for a range of  $K_{em}$  values around  $\sim 310 \pm 10 \text{ km s}^{-1}$ , the narrow components show the highest intensities together with narrow widths consistent with the spectral resolution of  $\sim 90 \text{ km s}^{-1}$ . Taking into account the position of the spots in the Doppler maps (i.e. orbital phase and velocity), the narrowness of the components and the presence of similar high excitation features in all the persistent LMXBs that we have studied (see Cornelisse et al. 2008) we associate these features with X-ray reprocessing from the irradiated hemisphere of the donor.

It is also noteworthy that we have a tentative detection of the N III and C III components within the Bowen blend in the rest frame of the companion star (left panel in Fig. 5). The weakness of these lines is probably due to the reduced number of spectra. We only cover one orbit and at least two orbits of data are usually required to clearly detect these transitions (e.g. see Casares et al. 2006). However, the He II emission lines are very strong in this system compared to others previously studied and show narrow components that provide us with the opportunity to measure  $K_{em}$ . It is especially interesting to note that EXO 0748-676 is the only system in the Bowen survey where He II  $\lambda 4542$  is as strong as the Bowen blend. He II  $\lambda 4686$  emission from the donor was also reported by Steeghs & Casares (2002) in Sco X-1, with a  $K_{em}$  value similar to that obtained from the Bowen lines. However, in other bright systems where high signal-to-noise studies have been performed (e.g. X1822-371 Casares et al. 2003) no He II emission from the donor was found.

## 5 SYSTEM PARAMETERS

EXO 0748-676 offers important advantages with respect to other persistent LMXBs. The binary inclination is a known function of the mass ratio owing to the X-ray eclipses (Hynes et al. 2006). For instance,  $i = 82^\circ$  yields  $q = 0.12$ , whereas  $i = 75^\circ$  implies  $q = 0.4$ . Moreover, since X-ray eclipses and X-ray bursts from the NS surface are observed, the NS must be visible, and hence the disc opening angle  $\alpha$ , which obscures part of the irradiated face of the donor, is also related to the inclination through  $\alpha \leq 90^\circ - i$ . Therefore for a given  $q$ , the inclination angle and an upper limit to  $\alpha$  are set. This is very useful in order to compute the K-correction. Emission lines formed on the inner hemisphere of the donor star as a result of X-ray reprocessing only provide a lower limit ( $K_{em}$ ) to the true  $K_2$ -velocity. In Muñoz-Darias et al. (2005) we model the deviation between the light-center of the reprocessed lines and the center of mass of a Roche lobe filling star in a persistent LMXB, including screening effects by a flared accretion disc (i.e. the K-correction). We find that this correction depends on  $q$ ,  $\alpha$  and weakly on the orbital inclination. We now apply the K-correction to EXO 0748-676 as a function of  $q$ , including the above limits on  $q$  and  $i$ .

### 5.1 The mass of the neutron star

Fig. 6 shows the lower limit to the NS mass as a function of  $q$  obtained from  $K_{em} = 300 \text{ km s}^{-1}$  (lower solid line). Assuming

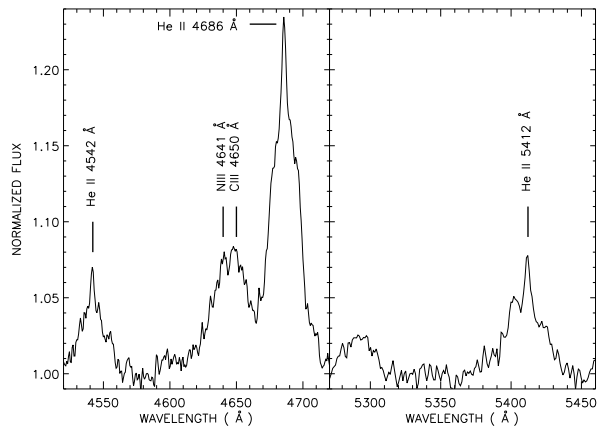


**Figure 5.** Normalized average spectrum of EXO 0748-676 in the rest frame of the companion (using  $K_{em} = 300 \text{ km s}^{-1}$ ). Note the narrow components standing out in He II  $\lambda 4542$ ,  $\lambda 4686$  and  $\lambda 5412$ .

$K_1 \sim 100 \text{ km s}^{-1}$  (favored by the diagnostic diagram) we obtain  $q \lesssim 0.35$ , in agreement with Hynes et al. (2006). On the other hand, if we use the maximum K-correction ( $\alpha = 0^\circ$ ) and the upper limit  $K_{em} = 320 \text{ km s}^{-1}$  we obtain an upper limit to the NS mass (upper solid line in Fig. 6). Meyer & Meyer-Hofmeister (1982) suggest that, even in the absence of irradiation, accretion discs in LMXBs have  $\alpha \gtrsim 6^\circ$ , which is also consistent with the results by D’Avanzo et al. (2006) for Cen X-4 in quiescence. Applying the the K-correction with  $\alpha \gtrsim 6^\circ$  and  $K_{em} = 320 \text{ km s}^{-1}$  we obtain a less conservative upper limit represented by the dotted-dashed line in Fig. 6.

Pearson et al. (2006) favored  $q = 0.34$  y  $M_1 \approx 1.35 M_\odot$  by fitting gas stream trajectories to the extended spot observed in the He II  $\lambda$ Doppler map. This pair of values, which is marked by the dotted line in Fig. 6, is not consistent with our results. Conversely, our results are consistent with those derived by Özel (2006), which are represented by the grey region in Fig. 6. Nevertheless, our values are also consistent with the presence of a canonical NS with  $\sim 1.4 M_\odot$  in EXO 0748-676. However, for this case to work we need  $q \leq 0.24$

### 5.2 The nature of the donor star

The parameter constraint for EXO 0748-676 are consistent with a main sequence star and clearly a giant star cannot fit within the 3.8 h Roche lobe. Faulkner et al. (1972) showed that the mean density ( $\bar{\rho}$ ) of a Roche lobe-filling companion star is determined solely by the binary period  $P$ :

$$\bar{\rho} \cong 113 P_h^{-2} \text{ g cm}^{-3}$$

where  $P_h$  is the orbital period in hours. For EXO 0748-676, with  $P_h = 3.82$  hours, we obtain  $M_2 \sim 0.42 M_\odot$  (Cox 2000), which defines the right dashed line in Fig. 6 through  $M_1 = M_2/q$ . Combining this relation with the lower, thick solid line we obtain  $M_1 \geq 1.5 M_\odot$  for the case of a main sequence donor.

Alternatively, the donor star could have evolved before the onset of mass transfer. For this to happen within a Hubble time, the binary must have experienced an episode of unstable mass transfer with  $q > 1$  in a thermal time scale. The final product of this scenario is a LMXB formed by a donor star with an evolved nucleus transferring material onto a NS. Schenker & King (2002) have computed com-

panion star masses versus the orbital period for the limiting case of a nearly all helium nuclei. Using their relation for the case of EXO 0748-676 we obtain  $M_2 \gtrsim 0.16 M_\odot$  which yields the left dashed line in Fig. 6. Altogether, the allowed region in the  $M_1 - q$  space of parameters yields  $1 M_\odot \leq M_1 \leq 2.4 M_\odot$  and  $0.11 \leq q \leq 0.28$  whereas a plausible  $\alpha \geq 6^\circ$  implies  $M_1 \leq 2.0 M_\odot$ . It is also interesting to consider a limiting case with  $q = 0.28$ ,  $\alpha = 6^\circ$  and  $K_{\text{em}} = 320 \text{ km s}^{-1}$  together with  $K_1 \sim 100 \text{ km s}^{-1}$  from the diagnostic diagram. For this case we obtain  $q \geq 0.22$  and therefore  $M_1 \geq 1.3 M_\odot$ , favoring the main sequence scenario. However, we note that the unstable mass-transfer scenario was proposed to explain the observations in XTE J1118+480 (Haswell et al. 2002) and Cyg X-2 (Podsiadlowski & Rappaport 2000). More recently, Rodríguez-Gil et al. (2009) show that the mass of the companion star in the cataclysmic variable HS 0218+3229 is also in excellent agreement with the predictions of Schenker & King (2002).

## 6 CONCLUSIONS

We present the first dynamical determination of the NS mass in EXO 0748-676. Assuming that the narrow components detected within the He II  $\lambda 4542$ ,  $\lambda 4686$  and  $\lambda 5412$  emission lines arise from the irradiated hemisphere of the donor we measure  $K_{\text{em}} = 300 \pm 10 \text{ km s}^{-1}$  which results in  $1 M_\odot \leq M_1 \leq 2.4 M_\odot$  and  $0.11 \leq q \leq 0.28$ . On the other hand, the mass of the donor star is constrained to  $0.16 M_\odot \leq M_2 \leq 0.42 M_\odot$  through unstable mass-transfer/main sequence models. For the case of a main sequence donor we find  $M_1 \geq 1.5 M_\odot$ .

Our results are consistent with the Özel (2006) scenario and rule out other system parameters proposed by Pearson et al. (2006). However, our observations are also consistent with a canonical mass NS and more observations are required to further constrain the mass of the NS in EXO 0748-676. Recently, EXO 0748+676 has been reported to reach quiescence at  $R = 21.9$  after  $\simeq 22$  years of activity (Hynes & Jones 2008). This provides an excellent opportunity to measure the orbit of the companion star and determine the mass of the NS.

JC acknowledges support from the Spanish Ministry of Science and Technology through the project AYA2007-66887.DS acknowledges a STFC Advanced Fellowship. Partially funded by the Spanish MEC under the Consolider-Ingenio 2010 Program grant CSD2006-00070: First Science with the GTC. The use of the spectral analysis software package MOLLY written by Tom Marsh is acknowledged.

## REFERENCES

Casares J., 2009, Proceedings of the VIII Scientific Meeting of the Spanish Astronomical Society (SEA), in press  
 Casares J., Cornelisse R., Steeghs D., Charles P. A., Hynes R. I., O'Brien K., Strohmayer T. E., 2006, MNRAS, 373, 1235  
 Casares J., Steeghs D., Hynes R. I., Charles P. A., O'Brien K., 2003, ApJ, 590, 1041  
 Cornelisse R., Casares J., Muñoz-Darias T., Steeghs D., Charles P., Hynes R., O'Brien K., 2008, ArXiv e-prints, 801  
 Cornelisse R., Casares J., Steeghs D., Barnes A. D., Charles P. A., Hynes R. I., O'Brien K., 2007, MNRAS, 375, 1463  
 Cottam J., Paerels F., Mendez M., 2002, Nature, 420, 51

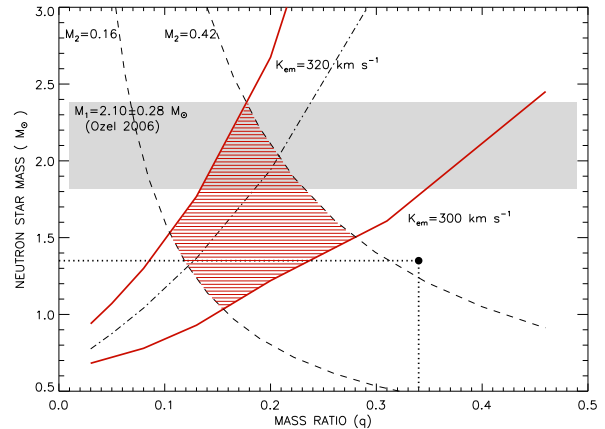


**Figure 6.**  $M_1$  vs  $q$  obtained from  $K_{\text{em}} = 300 \pm 10 \text{ km s}^{-1}$ . The solid lines represent the lower and upper limits to the NS mass for  $\alpha_{m,ax}$  and  $\alpha = 0^\circ$  respectively, whereas the dotted-dashed line corresponds to the upper limit for  $\alpha \geq 6^\circ$  (Meyer & Meyer-Hofmeister 1982). The grey region shows the mass range determined by Özel (2006) and the solid circle with dotted lines the values favored by Pearson et al. (2006). The dashed lines are obtained assuming that the donor is either a  $M_2 \sim 0.42 M_\odot$  main sequence star or it is considerably evolved before the onset of mass transfer. The shadowed region indicates our constraints on  $q$  and  $M_1$ .

Cox A., 2000, Allen's astrophysical quantities, S&T, 100, 72  
 D'Avanzo P., Muñoz-Darias T., Casares J., Martínez-Pais I. G., Campana S., 2006, A&A, 460, 257  
 Faulkner J., Flannery B. P., Warner B., 1972, ApJ, 175, L79+  
 Gottwald M., Haberl F., Parmar A. N., White N. E., 1986, ApJ, 308, 213  
 Haswell C. A., Hynes R. I., King A. R., Schenker K., 2002, MNRAS, 332, 928  
 Hynes R., Jones E., 2008, The Astronomer's Telegram, 1816, 1  
 Hynes R. I., Horne K., O'Brien K., Haswell C. A., Robinson E. L., King A. R., Charles P. A., Pearson K. J., 2006, ApJ, 648, 1156  
 Hynes R. I., Steeghs D., Casares J., Charles P. A., O'Brien K., 2003, ApJ, 583, L95  
 Marsh T. R., Horne K., 1988, MNRAS, 235, 269  
 Meyer F., Meyer-Hofmeister E., 1982, A&A, 106, 34  
 Muñoz-Darias T., Casares J., Martínez-Pais I. G., 2005, ApJ, 635, 502  
 Muñoz-Darias T., Casares J., Martínez-Pais I. G., 2008, MNRAS, 385, 2205  
 Özel F., 2006, Nature, 441, 1115  
 Parmar A. N., White N. E., Giommi P., Gottwald M., 1986, ApJ, 308, 199  
 Parmar A. N., White N. E., Giommi P., Haberl F., Pedersen H., Mayor M., 1985, IAU Circ., 4039, 1  
 Pearson K. J., Hynes R. I., Steeghs D., Jonker P. G., Haswell C. A., King A. R., O'Brien K., Nelemans G., Méndez M., 2006, ApJ, 648, 1169  
 Podsiadlowski P., Rappaport S., 2000, ApJ, 529, 946  
 Rodríguez-Gil P., Torres M. A. P., Gansicke B. T., Muñoz-Darias T., Steeghs D., Schwarz R., Hagen H.-J., 2009, A&A submitted  
 Schenker K., King A. R., 2002, Astronomical Society of the Pacific Conference Series, 261, 242  
 Schneider D. P., Young P., 1980, ApJ, 240, 871  
 Shafter A. W., Szkody P., Thorstensen J. R., 1986, ApJ, 308, 765  
 Steeghs D., Casares J., 2002, ApJ, 568, 273  
 Villarreal A. R., Strohmayer T. E., 2004, ApJ, 614, L121  
 Wolff M. T., Hertz P., Wood K. S., Ray P. S., Bandyopadhyay R. M., 2002, ApJ, 575, 384